Journal of Ceramic Processing Research. Vol. 7, No. 1, pp. 14~19 (2006)

J O U R N A L O F
Ceramic Processing Research

Injection molding of ultra-fine zirconia (Y-TZP) powders

Jie-sheng Luo[a], Zhong-zhou Yi[b], Bing Xiao[c], Yan Gao[a], Zhi-peng Xie[a,*], Jian-bao Li[a] and Yong Huang[a]
[a]*Department of Materials Science & Engineering, Tsinghua University, Beijing, 100084, China*
[b]*Chemistry Department of Honghe University, Yunnan 661100, China*
[c]*Zhongyuan Engineering College, Zhengzhou 450007, China*

Injection moldings of three types of ultra-fine zirconia powder were investigated. It was demonstrated that powder characteristics involving particle size, particle size distribution, particle shape and specific surface area significantly affect the optimal compositions of binders and ceramic powders, and the properties of sintered compacts. Investigation of the injection molding variables showed that an excessive barrel-deposited value may easily lead to defects in the de-bound and sintered bodies. It was also demonstrated that the microstructure of a sintered body can be affected by heating rates influencing grain growth, and that suitable heating rates to the high temperature sintering stage for the three powders are different.

Key words: Injection molding, zirconia powder, ceramic sintering.

Introduction

The Ceramic Injection Molding (CIM) technique has the ability to produce complex-shaped ceramic parts, with high production capacity and relatively high dimensional precision [1-3]. Fully tetragonal-stabilized zirconia with yttrium oxide (Y-TZP) in particular is a structural ceramic with excellent mechanical properties. This engineering ceramic, especially with grain sizes of nanometre or sub-micrometre range, can exhibit high strength and fracture toughness. Ceramic materials with extremely small grain sizes require a starting powder which is very fine with a narrow size distribution [4-6]. Therefore, injection molding of ultra-fine zirconia has received great attention in recent years [7-9].

In this study, injection molding of three types of ultra-fine Y-TZP powder was investigated. The characteristics of the three zircoina powders, involving particle size distribution and particle morphology were compared. The influence of powder characteristics on the composition of optimized pre-injection molding mixtures, consisting of ceramic powders and binders, and their influence on the properties of the final sintered parts were investigated. The effect of the barrel-deposited value on the injection molding of zirconia and the influence of heating rate to the final sinter temperature on the microstructure of sintered parts were also investigated.

*Corresponding author:
Tel : +86-10-6279-4603
Fax: +86-10-6279-4603
E-mail: xzp@mail.tsinghua.edu.cn

Experimental

Materials

Three different types of zirconia powder, designated A, B and C, all containing 3 mol% Y_2O_3, were used in this study. Powder A had an average particle size of 0.146 mm and a specific surface area of 8.21 m^2/g. Power B had an approximately average particle size similar to powder A, 0.124 μm, and a specific surface area of 9.70 m^2/g. Powder C had an average particle size of 0.085 μm and a specific surface area of 14.72 m^2/g.

The binders used in this investigation were paraffin wax (PW) as the major binder, and polyethylene (PE), polypropylene (PP), dibutyle phthalate (DBP) as assistant binders.

Procedure

The mixtures of organic binders and zirconia powder with various solid loading levels were kneaded in a twin screw kneader (SK-160, ShangHai Rubber Machinery, China) at a temperature of 160-170 °C for a period of 5 minutes. After a 24 h interval the mixtures were compounded again at 130 °C for 10 minutes. The specimens were made using an injection molding machine (JPH30 C/E, Qinchuan HengYl Plastics Machinery Co. Ltd, China) to nominal dimensions of $4 \times 6 \times 60$ mm. A barrel temperature series of 140-160-165-170 °C from feed to nozzle was used. The hold pressure and hold time were 25 MPa and 3.0 s, respectively. The cool time was 3.0 s and the molding temperature was 45 °C.

The as-molded compacts had their binders removed in a muffle furnace using the following schedule:

increasing the temperature at 10 Kh^{-1} from room temperature to 600 °C and held for 2 h. The sintering of a debound body was done in a chamber furnace (LHT04/17, Nabertherm, Germany), at either 1550, 1450, or 1400 °C for mixtures A, B and C, respectively.

Measurements

The rheological behavior of the mixtures was characterized at a fixed temperature of 170 °C using a capillary rheometry (canton, Instron model 3211, England) over a shear rate range from 0.1 to 1600 s^{-1}. The surface appearance of the green parts was observed by a stereoscopic microscope (KH-1000, HIROX, Japan). The flexural strength of sintered bars was measured using a three-point bending method, with a span of 30 mm. Bar surfaces were polished on a grinding machine, and the final dimensions of the samples were $3 \times 4 \times 42$ mm. The fracture toughness was determined using a specimen with a single edge-notched girder test (SENG). The specimens, with nominal dimensions of $3 \times 4.5 \times 36$ mm, contained a notch of 2 mm depth and 0.1 mm width positioned at the midpoint on the 4.5×36 mm surface.

Results and discussion

Powder characteristics and their influence on injection molding

Ceramic injection molding involving the rheological behavior of the feedstock, properties of the molded body, debinding and sintering are largely affected by the characteristics of the starting powder including particle size, size distribution, particle shape and the presence of any powder agglomerates.

The measured particle size distributions of the three powders used in this study are shown in Fig. 1. Powder A had a wide particle size distribution, powder B had a narrower particle size distribution and Powder C had the narrowest particle size distribution. It is evident that

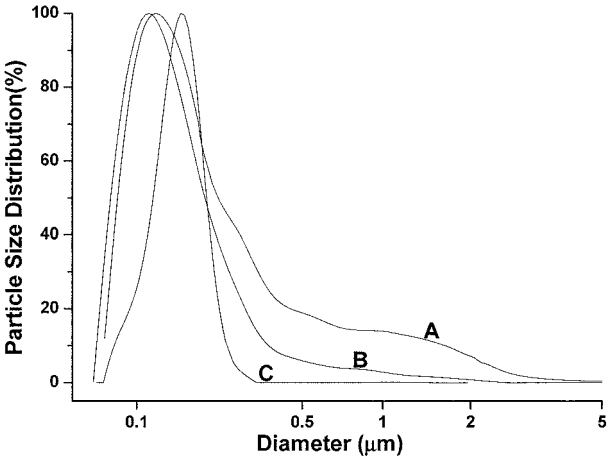

Fig. 1. Particle size distribution of zirconia powders A. B. and C.

our measurements for the particle size distributions of powders A and B are consistent with the commercially-given data about the mean particle sizes of powders A and B, which were 0.146 μm and 0.124 μm, respectively. The particle size distribution of powder C does not coincide with the data given about the mean particle size of powder C, 0.085 μm. From our data it can be seen that the average particle size of powder C is close to 0.2 μm, which when compared with Fig. 2(c) may be the result of poor particle separation prior to our measurements. Fig. 2 presents the transmission electron microscopy results of the three types of ultra-fine zirconia powders, showing the distinguishing features and morphology of the particles in the three powders. It is evident that the sizes of different particles are not similar and the shapes of particles are irregular in powder A, Fig. 2(a), and that the sizes of different particles are similar to those of powder B where the shapes of particles are spherical, see Fig. 2(b). Considerable powder agglomeration can be seen in Fig. 2(c), which proved that this powder agglomeration lead to the different size measurements for the particle size

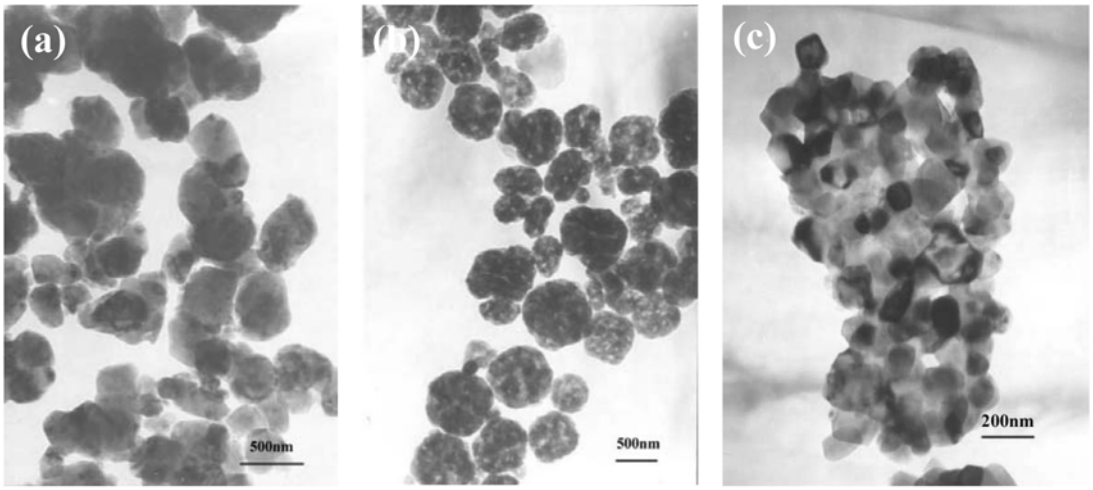

Fig. 2. TEM of zirconia powders used in current investigation (a) Powder A (b) Powder B (c) Powder C.

Table 1. Optimal batch compositions for different powders studied

Feedstock Type	Powder Type	Compositions (wt%)				
		Powder	PW	PP	PE	DBP
1#	A	89.22	5.06	1.40	1.30	3.02
2#	B	87.57	8.21	1.24	1.24	1.74
3#	C	84.70	10.10	1.53	1.53	2.14

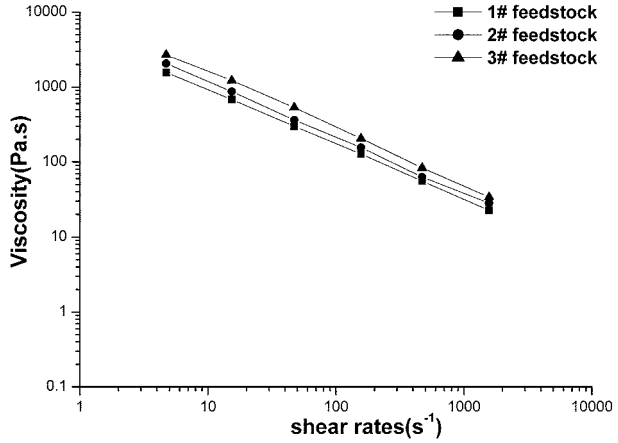

Fig. 3. Rheological behaviors of 1#, 2# and 3# feedstocks.

distribution and mean particle size in powder C.

The data in Table 1 shows the optimized compositions of the ceramic powder and binders for various batches. The compositions of ceramic batches were optimized with respect to the fluidity of feedstock, the properties of the green body and the properties of sintered body. Table 1 shows the various solid loadings and various binder contents results for the optimized batch compositions for the different ultra-fine zirconia powders. The optimized solid loading for powders A, B, C and content of PW in feedstocks prepared from powders A, B, C were 89.22 wt%, 87.57 wt%, 84.70 wt% and 5.2 wt%, 8.2 wt%, 10.1 wt%, respectively, with the remainder accounted for by the assistant binders.

Figure 3 shows the rheological behavior of various batches prepared from the mixtures with the compositions of ceramic powder and binders shown in Table 1. The three types of suspensions display similar rheological behavior and similar viscosity. It has been demonstrated that the fluidity of the three batches at a temperature of 170 °C, are suitable for injection molding.

Some mechanical and physical properties of sintered-injection molded parts produced from various powder batches are given in Table 2. The various samples were prepared from the optimized compositions of the ceramic powder and binder batches shown in Table 1. The flexural strength of sintered-injection molded parts prepared from batches A, B and C were 900.6 MPa, 990.3 MPa and 872.6 MPa, respectively. Compared with batches B and C, the sintered parts injection molded using batch A exhibit higher values of fracture toughness, 12.8 $MPa \cdot m^{1/2}$.

As demonstrated by the results presented in Table 2, it is evident that powder characteristics significantly influence the optimal powder-binder batch formulations and hence properties of the sintered specimens. As a result of the various characteristics of zirconia powders, various binder formulations are needed for the different powders to achieve favorable injection molding, debinding and improve the properties of molded and sintered bodies. Various solid loadings were utilized for the different powders owing to the characteristics of the various zirconia powders. In principle, a desired powder-polymer suspension for CIM requires a relatively high solid concentration with the suspension viscosity as low as possible at a given temperature. Both requirements ensure a high green-shape density with a high degree of green microstructural homogeneity and of compact-structural integrity. Meanwhile, suspensions with relatively high solid loadings have a low content of binder, and this may facilitate binder removal during debinding. Powder A has a high packing efficiency owing to its wide particle size distribution. Powder C which has a narrow particle size distribution and small particle size contains particle agglomerates resulting in a low packing efficiency which requires high contents of paraffin wax acting as a major filler as well as surfactant.

The characteristic of zirconia powder leads to the different properties of sintered parts prepared from different powders. The average grain sizes of sintered compacts shown in Figs. 4(b), 5(b), and 6(a) are about

Table 2. Properties of sintered compacts injection moulded from Powder A, B and C

Powder type	Flexural strength (MPa)	Fracture toughness ($MPa \cdot m^{1/2}$)	Density (g/cm^3)	Linear shrinkage (%)
A	900.6 ± 80.2	12.8 ± 2.01	6.04	14.7
B	990.3 ± 68.6	12.1 ± 2.48	6.04	18.4
C	872.6 ± 60.8	12.0 ± 2.16	6.06	22.0

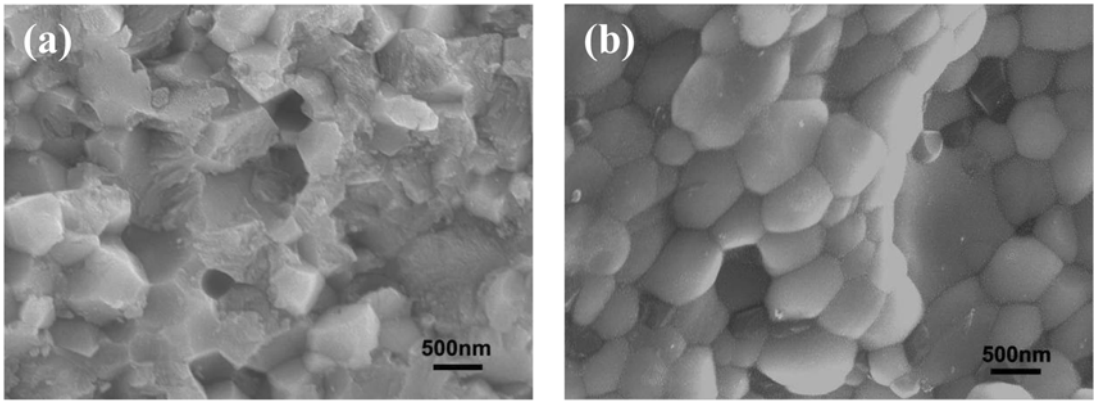

Fig. 4. The fracture surface of sintered parts prepared from powder A with various sintering rates (a) 1 K·minute^{-1}, (b) 2 K·minute^{-1}, from 1000 °C to 1550 °C

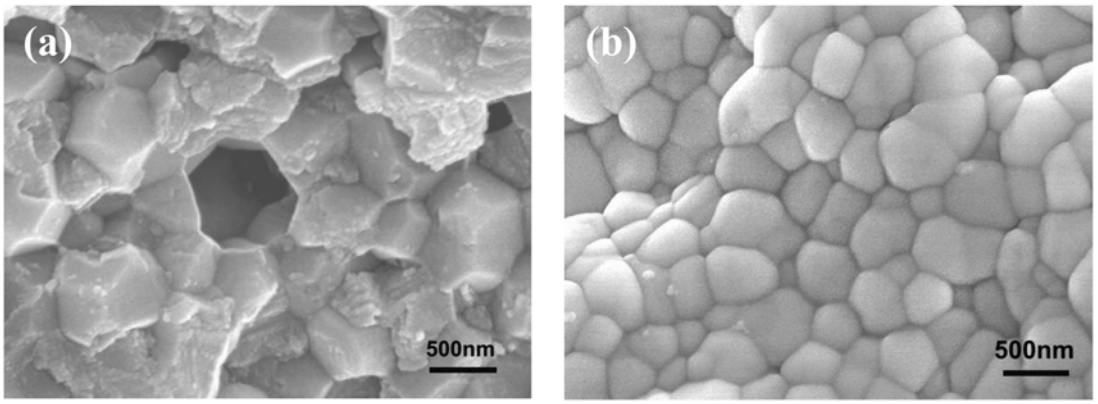

Fig. 5. The fracture surface of sintered parts prepared from powder B with various sintering rates (a) 1 K·minute^{-1}, (b) 2 K·minute^{-1} from 1000 °C to 1450 °C.

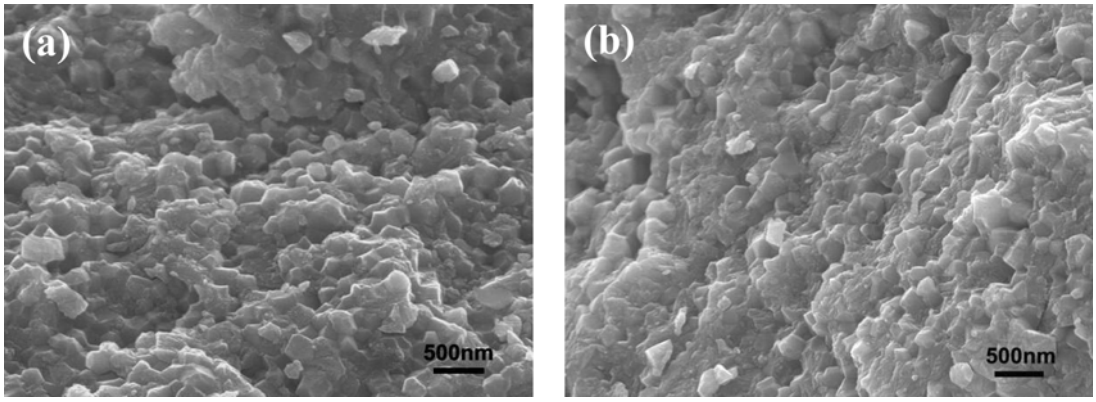

Fig. 6. The fracture surface of sintered parts prepared from powder C with various sintering rates (a) 1 K·minute^{-1}, (b) 2 K·minute^{-1}, from 1000 °C to 1400 °C.

490 nm, 370 nm and 230 nm, respectively. The sintered parts prepared from powder B exhibit the highest flexural strength because of the smaller grain size compared with parts from powder A. Although powder C has the smallest particle size, it is suggested that the powder agglomerates, and hence poor uniformity in batch C leads to the lowest flexural strength of sintered parts prepared from C. The sintered parts prepared from batch C have the biggest linear shrinkage as a result of the lowest ceramic solid loading and the highest binder content, and yet achieve the highest density. Sintered parts using batch A had the highest fracture toughness, because the large tetragonal phase-grain size enabled the tetragonal-to-monoclinic transformation to assist in developing the toughness.

Influence of process parameters on properties

It has widely been considered that optimization of molding variables in the injection molding operation should minimize the occurrence of distortion and begin

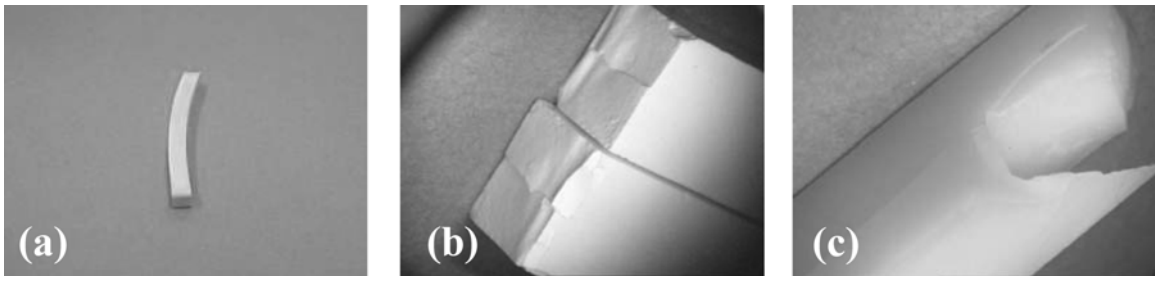

Fig. 7. Typical flaws result from using a larger barrel deposited value (a) warp in sintered sample (b) layered defects in debound body (c) crack in sintered body.

to facilitate dimensional control. Defects such as voids and cracks were found in ceramic injection molded products when the molding variables, especially barrel-deposited value, were not properly tuned. The barrel-deposited value is the distance between the front-end of the screw and the ejection nozzle. The diameter of the screw was 18 mm, and the maximum barrel-deposited value was 100 mm. The cracks introduced during molding operations became increasingly apparent at the subsequent stages of debinding and sintering. As is known, the integrity of molded samples is prone to be destroyed by using a small barrel-deposited value. Fig. 7. shows the typical flaws in a de-bound body and a sintered body which result from using a larger barrel deposited value. The size of the molded bars is about $5.80 \times 4.60 \times 43.0$ mm. Generally, the optimal barrel-deposited value of the bars was 45 mm, using a mould with eight cavities. The bars shown in Fig. 7 were injected using 48 mm as the barrel-deposited value. Fig. 7(a) shows the warping deformation of sintered samples fabricated at a larger barrel deposited value. Fig. 7(b) and Fig. 7(c) show the layered defects in the inner de-bound body and a crack in the section of a sintered section body as a result of using a larger barrel-deposited value. Larger barrel-deposited values often result in excessive feedstock injected into the constrained mold cavity. So, it is believed that a greater residual stress is introduced in the green bodies when a larger barrel-deposited value is utilized in the molding operations. Then, warp and layered defects would be found in the de-bound body, and especially in the sintered body. From this study it is also clear that a suitable barrel-deposited value is related to the mold cavity.

Influence of injection molded compact sintering behavior on microstructure

It is generally recognized that the densification of a green compact depends strongly on the sintering temperature and the heating rate to the sintering temperature. The influence of heating rate on the injection molding of ultra-fine zirconia powders was investigated by observing the microstructure of sintered samples prepared from different zirconia powders with various heating rates to the high temperature sintering temperature. The fracture surface of sintered compacts that were prepared from powder A with heating rates of 1 K·minute^{-1} and 2 K·minute^{-1} from 1000 °C to 1550 °C are shown in Figs. 4(a) and (b), respectively. Figs. 5(a) and (b) show the fracture surface of sintered compacts that were prepared from powder B with heating rates of 1 K·minute^{-1} and 2 K·minute^{-1} 1000 °C to 1450 °C, respectively. Figs. 6(a) and (b) show the fracture surface of sintered compacts that were prepared from powder C with heating rates of 1 K·minute^{-1} and 2 K·minute^{-1} from 1000 °C to 1400 °C, respectively. The various final sintering temperatures were determined by, and optimized for, the characteristics of the various powders, and the injection molding formulation and conditions used to form the green compacts.

From Fig. 4, 5 and 6, it is evident that the heating rate to the high temperature sintering stage strongly affects the microstructure of sintered compacts. Figs. 4(a) and 5(a) indicate that the rupture of sintered compacts occurs through some grains. This behavior demonstrates that excessive grain growth has occurred in the sintered compacts when 1 K·minute^{-1} is utilized for powders A and B to reach the high temperature sintering stage. However, Figs. 4(b) and 5(b) demonstrate that the rupture of sintered compacts occurs along the crystal boundaries when a heating rate of 2 K·minute^{-1} is used for powders A and B. The average grain sizes of sintered compacts shown in Figs. 4(b) and 5(b) are about 490 nm and 370 nm, respectively. Powder C differs from powders A and B. From Fig. 6(b), it is evident that grain growth arises easily in the sintered compact. It suggests that a heating rate of 2 K·minute^{-1} is excessively fast for grain growth in powder C, and 1 K·minute^{-1} is suitable. The average grain size of sintered compacts from batch C shown in Fig. 6(a) is about 230 nm.

Summary

Influences of powder characteristics, molding variables (ie. barrel-deposited value) and sintering behaviors on injection molding of ultra-fine zirconia powders were investigated. The study demonstrates that particle size, particle size distributions, particle shape and powder agglomerates affect the compositions of the binder-

mixture and final formulation that is suitable for injection molding. A small particle size, a narrow particle size distribution and powder agglomerates lead to low solid loading and a high content of paraffin wax, but the best density and fracture toughness. Powder characteristics also affect the properties of sintered samples including flexural strength, fracture toughness, density and linear shrinkage. Typical defects such as warp deformation and cracks, are prone to be found in the de-bounded body and sintered bodies when an excessive barrel-deposited value is used in the molding operation. Also the heating rate to the high temperature strongly effects the final microstructure of the sintered compacts. With a heating rate of 1 K·minute^{-1} excessive grain growth was found in the specimens prepared from powders A and B. A heating rate of 2 K·minute^{-1} was suitable for powders A and B, while, for powder C, 1 K·minute^{-1} was suitable.

Acknowledgements

This work was supported by the National Nature Science Foundation (NSF) of China and the National Key Basic Research Development Program (973 Program, G. No. 2000067204-01) of China.

References

1. R.M. German, in Proceeding of Powder Injection Molding, 1990, Metal Powder Industries Association.
2. M.J. Edirisinghe, and J.R.G. Evans, Materials section, Int. J. High Ceram. 2 (1986) 1-31.
3. R.M. German, K.F. Hens, and S.T. Lin, Am. Ceram. Soc. bull 70 (1991) 1294-1302.
4. A.H. Heuer, Am. Ceram. Soc., Columbus, OH (1981) 98-115.
5. M.J. Mayo, Int. Mat. Rev. 41 (1996) 85-115.
6. J.J. Blandin, A. Varloteaux, and B. Baudelet, in Proceedings of the Risoe International Symposium on Metallurgy and Materials Science, Structural Ceramics Processing, Microstructure and Properties, 1990, p. 199-204.
7. J.H. Song, J.R.G. Evans, Ceram. Int. 21 (1995) 325-333.
8. J.H. Song, J.R.G. Evans, J. Rheol. 40 (1996) 131-152.
9. Lin. Samuel I-En, Ceram. Int. 27 (2001) 205-214.